Magnetic Resonance Imaging 58 (2019) 135–142

Contents lists available at ScienceDirect

Magnetic Resonance Imaging

journal homepage: www.elsevier.com/locate/mri

Original contribution

MRI estimates of brown adipose tissue in children – Associations to adiposity, osteocalcin, and thigh muscle volume

Jonathan Andersson[a,*], Josefine Roswall[b,c], Emma Kjellberg[c], Håkan Ahlström[a,d], Jovanna Dahlgren[c,1], Joel Kullberg[a,d,1]

[a] Section of Radiology, Department of Surgical Sciences, Uppsala University, Uppsala, Sweden
[b] Department of Pediatrics, Hallands Hospital Halmstad, Halmstad, Sweden
[c] Department of Pediatrics, Institute of Clinical Sciences, Sahlgrenska Academy at University of Gothenburg, Gothenburg, Sweden
[d] Antaros Medical, Mölndal, Sweden

ARTICLE INFO

Keywords:
Brown adipose tissue
Magnetic resonance imaging
Adiposity
Osteocalcin
Muscle volume
Quantitative MRI

ABSTRACT

Context: Brown adipose tissue is of metabolic interest. The tissue is however poorly explored in children.
Methods: Sixty-three 7-year old subjects from the Swedish birth-cohort Halland Health and Growth Study were recruited. Care was taken to include both normal weight and overweight children, but the subjects were otherwise healthy. Only children born full term were included.

Water-fat separated whole-body MRI scans, anthropometric measurements, and measurements of fasting glucose and levels of energy homeostasis related hormones, including the insulin-sensitizer osteocalcin, were performed. The fat fraction (FF) and effective transverse relaxation time (T_2*) of suspected brown adipose tissue in the cervical-supraclavicular-axillary fat depot (sBAT) and the FFs of abdominal visceral (VAT) and subcutaneous adipose tissue (SAT) were measured. Volumes of sBAT, abdominal VAT and SAT, and thigh muscle volumes were measured.
Results: The FF in the sBAT depot was lower than in VAT and SAT for all children. In linear correlations including sex and age as explanatory variables, sBAT FF correlated positively with all measures of adiposity ($p < 0.01$), except for VAT FF and weight, positively with sBAT T_2* ($p = 0.036$), and negatively with osteocalcin ($p = 0.017$). When adding measures of adiposity as explanatory variables, sBAT FF also correlated negatively with thigh muscle volume ($p < 0.01$).
Conclusions: Whole-body water-fat MRI of children allows for measurements of sBAT. The FF of sBAT was lower than that of VAT and SAT, indicating presence of BAT. Future studies could confirm whether the observed correlations corresponds to a hormonally active BAT.

1. Introduction

The adipose tissue in humans can be crudely divided into two different types; brown (BAT) and white (WAT). BAT dissipates chemical energy as heat when thermogenically active, a process known as non-shivering thermogenesis, as opposed to the shivering thermogenesis of muscles. This dissipation of energy might protect against fat accumulation in energy storing WAT [1]. In infants, BAT is found mainly as an interscapular depot, but also in the cervical-supraclavicular-axillary region amongst other regions. However, with age the interscapular depot vanishes or decreases significantly in size, and the cervical-supraclavicular-axillary depot becomes the main location of BAT, herein denoted sBAT. In this depot, brown adipocytes are interspersed as clusters between unilocular white adipocytes [2]. Studies in adults have shown a negative association between BAT activity and adiposity [3,4]. There is optimism that the properties of BAT could be used to counteract overweight and obesity [5].

In humans WAT is an active endocrine organ which secretes

Abbreviations: BAT, brown adipose tissue; WAT, White adipose tissue; sBAT, cervical-supraclavicular-axillary fat depot; FF, fat fraction; T_2*, effective transverse relaxation time; WHtR, waist-to-height ratio; VAT, visceral adipose tissue; SAT, subcutaneous adipose tissue

* Corresponding author at: Section of Radiology, Department of Surgical Sciences, Uppsala University, MRT, Entrance 24, Uppsala University Hospital, SE-751 85 Uppsala, Sweden.
E-mail addresses: jonathan.andersson@surgsci.uu.se (J. Andersson), josefine.roswall@regionhalland.se (J. Roswall), emma.kjellberg@gu.se (E. Kjellberg), hakan.ahlstrom@akademiska.se (H. Ahlström), jovanna.dahlgren@gu.se (J. Dahlgren), joel.kullberg@radiol.uu.se (J. Kullberg).
[1] These authors contributed equally to this work.

https://doi.org/10.1016/j.mri.2019.02.001
Received 20 December 2018; Received in revised form 18 January 2019; Accepted 4 February 2019

adipokines, such as adiponectin and leptin. There is support that these hormones play a role in energy balance, insulin sensitivity, and fat metabolism [6]. Furthermore, in rodents BAT plays an endocrine role that differs from that of WAT, and there are indications that the same is true for humans [7]. In adult humans, BAT has been shown to be highly insulin sensitive [8]. By [^{18}F]-fludeoxyglucose (^{18}F-FDG) positron emission tomography (PET)/computed tomography (CT) scanning of adults, it has been shown that cold exposure activation of BAT increase whole-body glucose disposal and insulin sensitivity [9].

Studies suggest that BAT is mainly regulated by sympathetic neurons from several hypothalamic nuclei which are centrally stimulated by e.g. leptin and bone proteins [10,11]. On the other hand, it has been shown in humans that peripheral stimulation of BAT is exerted by cold [9], and in mice by e.g. adiponectin [12].

Certain hormones produced by the skeletal muscle may promote the recruitment of BAT [13]. In studies on rodents, it has been found that endurance exercise training stimulates the recruitment of brown-like adipocytes [13–15]. However, this effect has not been found in humans [16,17]. On the other hand, positive correlations between muscle quantity and BAT activity in humans have been reported in children and adolescents [18] as well as in adults [19].

Osteocalcin is a hormone produced by bone cells and is a marker of osteoblast activity and bone formation [20]. In mice it has been shown that osteocalcin is, in its undercarboxylated form, released into the blood stream and influences glucose metabolism by beta cell proliferation, increasing insulin secretion and by increasing adiponektin and thus augmenting insulin sensitivity in muscle and adipose tissue [21]. In mice, the secretion of osteocalcin is stimulated by leptin [22] as well as insulin [21]. Moreover, in mice it has been shown that osteocalcin is produced in BAT [23]. In vitro models have shown that osteocalcin stimulates thermogenesis in brown adipocytes [24]. In human cell cultures, the secretion of osteocalcin has been observed to be stimulated by adiponectin [25], but adiponectin also exert a direct effect on BAT to reduce energy expenditure. In young adults, osteocalcin has been shown to be negatively related to BMI and waist circumference [26].

To characterize human BAT with non-invasive methods is challenging. The pioneering, and still most widely used, method for estimating BAT activity in humans is PET, using ^{18}F-FDG as the radiotracer. [4,27–29]. An alternative imaging method, free from ionizing radiation, is magnetic resonance imaging (MRI). The lack of ionizing radiation is especially useful for studies on children, or in longitudinal studies, since the radiation the subjects otherwise would be exposed to is considered potentially harmful. By acquiring gradient echoes at multiple echo times, it is possible to perform water-fat separated MRI. In addition to images of the water and fat signal components, it is also possible to use the gradient echoes to calculate fat fraction (FF), i.e. the percentage of the signal originating from fat, and effective transverse relaxation time (T_2*), a measure of how quickly the signal declines.

Differences in FF and T_2* between BAT and WAT could be used to differentiate and characterize the two tissues [30–32]. The FF and T_2* in BAT is lower than in WAT in humans, likely because of differences in mitochondrial abundance, triglyceride content, and vascularization [30]. In adult humans, a higher FF and T_2* in the sBAT depot has been found to be associated with less cold activated BAT [33,34]. In these studies, dynamic ^{18}F-FDG PET scanning was used to quantify glucose uptake rate of the sBAT depot during cooling. In [33], the glucose uptake rate of sBAT correlated linearly with its FF measured during ambient temperatures (R^2 = 0.39) and during cooling (R^2 = 0.42), and also with T_2* (R^2 = 0.43 respectively R^2 = 0.63). In [34], the difference between the glucose uptake rate of sBAT and that of a reference WAT region correlated linearly with the FF of sBAT measured during ambient temperatures (R^2 = 0.56). In contrast, another study [35] found no correlations between the FF or T_2* of sBAT and different measurements of the depot using ^{18}F-FDG PET during individualized cooling.

In this study measurements (FF, T_2* and volumes) of sBAT using water-fat separated MRI in children, a previously poorly explored group when it comes to BAT, were performed. Associations between the sBAT FF and the remaining sBAT measurements, body composition measured by MRI, anthropometric measurements, and energy homeostasis related blood measurements, including novel measurements when it comes to associations to BAT, were performed. The knowledge gained could contribute to metabolic research with long-term objectives including reliable non-invasive assessment of BAT amount, metabolic activity, and function.

2. Subjects and methods

2.1. Study participants

Subjects were recruited from the Swedish birth-cohort on healthy children Halland Health and Growth Study consisting of 388 children born full term, as previously described [36]. Out of these children, 200 dropped out before follow up when 6.6 years old, leaving 188 children. Eighty-seven of these were asked to be scanned using MRI, out of which 5 declined, leaving 82 participants. Those recruited for MRI scanning were selected to consist of equal parts normal weight and overweight/obese children based on their BMI at 5 years of age. For 12 of these children, only the abdomen was scanned, leaving a total of 70 children that underwent the whole-body MRI scanning. Out of these 70 children a total of 7 children showed water-fat swaps in the cervical-supraclavicular-axillary area that were judged as too severe for sBAT FF to be estimated. The remaining 63 children were included in this study.

2.2. Anthropometric measurements and serum sampling

At approximately age 6.6 years the children underwent anthropometric measures and blood sampling. This was performed year round. This was approved by the regional research ethics committee in Lund (study number 2014/531). Written consent was obtained from the parents involved as well as assent from all children to perform the examination.

The children were weighed in underclothes and measured to the nearest 0.1 kg on electronic step scales (Tanita WB-100MA, Tanita, Tokyo, Japan). Their height was measured to the nearest 0.1 cm with a wall mounted stadiometer (Hyssna M, Hyssna, Sweden). Waist circumferences were measured midway between the iliac crest and lowest rib after a gentle expiration. BMI and waist-to-height ratio (WHtR) were calculated. Using their BMIs, the children were categorized into weight-groups according to the cut-offs set out by Cole et al. [37]. Pubertal status was assessed according to the definition by Tanner and Whitehouse [38].

Blood was sampled after a night's fasting. Sampling was performed during the morning, typically between 8:00 AM and 9:30 AM. All blood samples were immediately centrifuged, and sera were frozen at −80 °C within 1 h.

Glucose was measured by an enzymatic method with hexokinase, and insulin was measured by an electrochemiluminescence immunoassay, both on a Cobas 6000 analyzer (Roche Diagnostics GmbH, Mannheim, Germany). The intra-assay coefficient of variation was 2.2% for glucose and 2.0% for insulin. Total osteocalcin was measured using an automated chemiluminescence immunoassay (IDS-iSYS N-MID® Osteocalcin, IDS Immunodiagnostic Systems Deutschland GmbH, Frankfurt am Main, Germany). Adiponectin concentrations were measured by ELISA (R&D System Inc., Minneapolis, MN, USA). Leptin concentrations were measured by RIA (Merck Millipore, Darmstadt, Germany). For coefficient of variations of these measurements at different concentrations, see Table S1 in the supplementary materials.

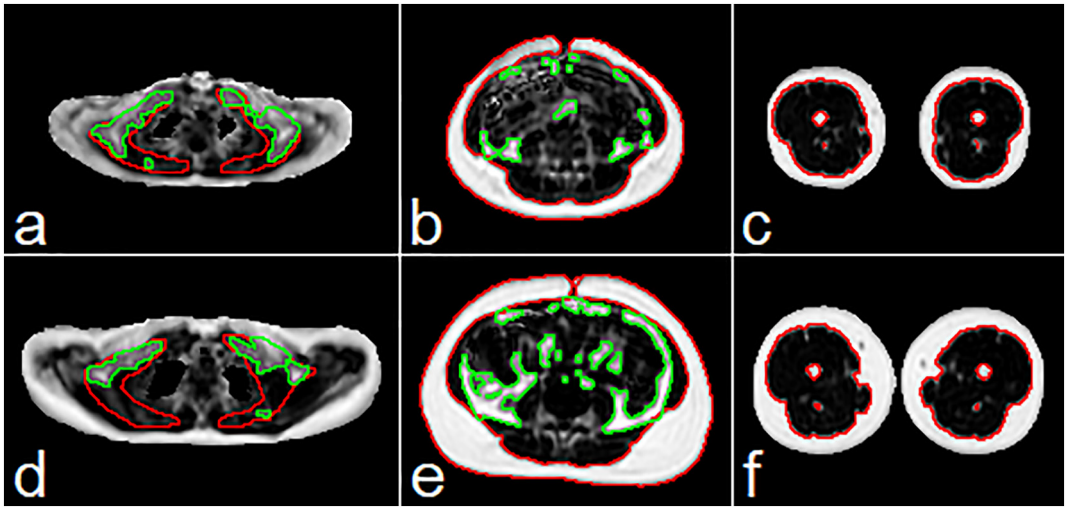

Fig. 1. Axial FF images showing different delineations used. In **a–c** a representative normal weight subject, in **d–f** a representative obese subject. Both subjects are females. In **a/d** images of the sBAT depot are shown. The red delineations were manually created. The green delineations, containing only voxels with a FF ≥ 30%, were used for measuring the sBAT volumes. In **b/e** images centered on the umbilicus are shown. The areas delineated in red were used for measuring the SAT volumes and the areas delineated in green were used for measuring the VAT volumes. In **c/f** images of thighs are shown. The areas delineated in red were used for measuring the thigh muscle volumes. (For interpretation of the references to colour in this figure legend, the reader is referred to the web version of this article.)

2.3. Magnetic resonance imaging

At approximately age 7 years the children were scanned using a whole-body MRI protocol. Scanning was performed year round. This was approved by the regional research ethics committee in Gothenburg (study number 375-15). Written consent was obtained from the parents involved. The children were informed about the procedure of the examination and gave their assent.

The scanning was performed at normal room temperature without cooling. The children could listen to audio or watch a video of their choice during the examination. The children were in supine position during scanning, and no sedation or anesthesia was used. On the day of the MRI examination the children had eaten a fat-free breakfast. The breakfasts were provided by the families at home. They had received written and oral instructions for the contents of the breakfast. All dairy products were prohibited, as well as eggs, meat, and fat containing toppings for sandwich/toast, e.g. peanut butter or chocolate. They were recommended white bread with jam, fruits, and juice.

The children were examined with a whole-body 3D fast spoiled gradient 6-echo sequence (IDEAL-IQ), using a 3.0 T clinical MR system (Discovery 750w, GE Healthcare, Waukesha, WI, USA), producing water, fat, FF, and T_2* images. A combination of a 19-elements head coil, 32-elements body coil, and a 36-elements peripheral vascular array was used. MRI was performed at 10 stations of 28 transversal slices each. At four stations images were acquired during breath hold, the children had been trained to hold their breath beforehand.

For most of the included subject the following scan parameters were used: repetition time = 6.2 ms, echo times = 0.9–4.6 ms, flip angle = 3°, echo train length = 3, receiver bandwidth = ± 111 kHz, field of view = 48 × 28.8 cm^2, acquisition matrix = 160 × 128, number of excitations = 0.69, parallel imaging (ARC) acceleration factor = 2 in both phase and slice direction, nominal resolution = 1.88 × 1.88 × 6 mm^3. The scan time per station was 13 s, with a total scan time of 10–12 min.

For 5 of the included subjects the some scanning parameters were slightly different, with the following parameters being the main divergence: field of view = 42 × 25.2 cm^2, acquisition matrix = 128 × 116, nominal resolution = 1.64 × 1.64 × 6 mm^3.

2.4. Segmentation and measurement of sBAT

A standardized manual delineation in the cervical-supraclavicular-axillary area was performed in a manner similar to that described in a previous publication [39]. The delineation mainly included the sBAT depot, but also the interscapular depot, which is much smaller than the sBAT depot in this age group. For simplicity, all the fat depots within the delineation are referred to as sBAT in this manuscript. Delineation was performed from the first axial slice above the heart to the last slice where the sBAT depot was visible.

For measuring the sBAT volume, only the voxels with a FF ≥ 30% (considered as likely BAT) within the delineation were included.

For measurements of FF and T_2* at first voxels with a FF ≥ 30% were segmented and thereafter eroded using a 6-neighborhood structural element to decrease the effect of partial volumes. The remaining voxels within the manual delineation were used for calculating the values. The mean FF was calculated, and T_2* was calculated as the inverse of the mean effective transverse relaxation rate.

The reason for setting the FF cutoff to 30% and not to 50% (as for visceral (VAT) and subcutaneous adipose tissue (SAT), see below) for the sBAT was that otherwise the resulting volume would in many cases be extremely small. In some cases no voxels would remain after erosion.

For an unbiased comparison of the FF of the sBAT depot to the FFs of VAT and SAT, measurements of sBAT FF were performed as above, but the FF cutoff was set to 50%. This was solely done for these comparisons. The resulting FFs are not presented or used in regressions.

An example of the manual delineation and the voxels used for volume measurement can be seen in Fig. 1a.

2.5. Segmentation and measurement of VAT and SAT

Measurements of VAT and SAT were centered on the umbilicus and spanned 162 mm in the feet-head direction. The body was segmented from the background using threshold levels determined slicewise using Otsu's method [40] on the sum of the water and the fat images. Arms were automatically removed by considering only the largest connected component. VAT and SAT were automatically segmented using the inside lean tissue filter [41], with voxels of FF ≥ 50% considered as adipose tissue. Bones and adipose tissue near the spine belonging to neither depot were manually removed. Errors of the automated method were manually corrected. The volumes were measured. Erosions were

performed separately for VAT and SAT using a 6-neighborhood structural element before FFs were measured as the mean in the remaining volumes. This erosion was performed to decrease the effect of partial volumes. T_2* was not measured due to poor quality. An example of the resulting volumes used for measuring volumes can be seen in Fig. 1b.

2.6. Segmentation and measurement of thigh muscles

Thigh muscle volumes were automatically measured. The volumes were measured over 96 mm in the feet-head direction, with the topmost slice of the volume manually defined as the slice below the bottommost slice in which the gluteus maximus muscle was visible. Background was removed in the same way as for the VAT and SAT measurements. The remaining voxles with a FF ≥ 50% were removed, and finally only the two largest remaining connected components (the muscles of the two thighs) were kept. Volumes were measured. A resulting segmentation can be seen in Fig. 1c.

2.7. Statistics

The FF of sBAT was compared to that of VAT and SAT. Correlations between sBAT FF and other parameters were studied using multiple linear regressions, with adjustment for age at the time of the MRI examination and sex. Multiple linear regressions were also performed with the addition of adjustment for adiposity by means of BMI or SAT volume. The reasons for selecting these two measurements for representing adiposity were that BMI is a common anthropometric measurement, and SAT volume, with the exception of sBAT volume, was observed to be the volumetric MRI measurement with the highest correlation to sBAT FF. p-Values < 0.05 were considered statistically significant.

3. Results

Sixty-three children underwent whole-body MRI scans at ages 6.97–7.47 years. Thirty-four of the children were males, and 29 females. Two children had thinness, 38 were normal weight, 19 were overweight, 3 were obese, and one was morbidly obese. They were all found to be prepubertal. With a couple of exceptions, they were all of Western European decent. Characteristics of the included children are shown in Table 1. In Tables S2 and S3 in the supplementary materials the characteristics for groups split by sex respectively weight class are shown. The highest measured sBAT FF was lower than the lowest measured FF in both SAT and VAT. This was true both when setting the sBAT cutoff to 30%, as can be seen in Table 1, and also when setting the cutoff to 50%.

The results of the multiple linear regressions for sBAT FF against the other parameters, with age and sex as additional explanatory variables, are shown in Table 2. The same regressions, but with sBAT volume replacing sBAT FF can be found in Table S4a and b in the supplementary materials. The different measurements reflecting adiposity, with the exception of weight and VAT FF, but including leptin, correlated positively with sBAT FF. Additionally, sBAT T_2* correlated positively and osteocalcin correlated negatively with sBAT FF.

The results of the multiple linear regressions for sBAT FF against thigh muscle volume and blood serum analyses, with age, sex, and BMI as explanatory variables, are shown in Table 3. The results of the same regressions, but with SAT volume as an explanatory variable instead of BMI, are shown in Table 4. In these regressions, thigh muscle volume and osteocalcin correlated negatively with sBAT FF, while no correlation was found between leptin and sBAT FF. Additionally, the same regressions, but with SAT FF replacing BMI or SAT volume as an explanatory variable, can be found in Table S5a, and the same regressions with both SAT FF and SAT volume as explanatory variables can be found in Table S5b, both in the supplementary materials.

Selected individual coefficient plots [42] are shown in Fig. 2.

Table 1
Characteristics of the included subjects (n = 63).

Variable	Mean	Standard deviation	Range
Age [years]	7.15	0.12	6.97–7.47
Weight [kg]	25.3	4.0	18.6–35.0
Height [cm]	122.4	4.8	114.0–131.5
WC [cm]	56.7	5.0	48.5–71.5
BMI [kg/m^2]	16.8	2.1	13.0–22.4
WHtR	0.464	0.037	0.396–0.581
MRI data			
sBAT FF [%]	57.2	5.2	44.8–68.6
sBAT T_2* [ms]	8.7	2.7	3.1–17.2
sBAT volume [l], n = 62	0.048	0.026	0.017–0.181
sBAT volume [l], n = 61[a]	0.046	0.019	0.017–0.109
VAT FF [%], n = 61	86.1	1.9	80.6–89.8
VAT volume [l], n = 62	0.19	0.15	0.05–0.97
VAT volume [l], n = 61[a]	0.17	0.11	0.05–0.53
SAT FF [%], n = 61	88.8	2.9	80.3–93.3
SAT volume [l], n = 62	1.21	0.60	0.33–3.07
Thigh muscle volume [l], n = 62	1.13	0.18	0.83–1.55
Serum analyses			
Insulin [pmol/l], n = 56	32	14	6–72
Glucose [mmol/l], n = 53	4.54	0.49	3.0–5.3
Osteocalcin [μg/l], n = 61	113	32	20–192
Adiponectin [mg/l], n = 61	10.4	5.1	2.1–29.8
Leptin [μg/l], n = 60	5.3	2.8	2.0–15.4

In case data was not available for all subjects, the number of included subjects is noted.
[a] Excluding one extreme outlier, same subject in both cases.

4. Discussion

To our knowledge, this is the first study to show a negative correlation between the sBAT FF and the serum osteocalcin concentration in humans. The correlation was found both with and without correction for adiposity. This finding led us to hypothesize that osteocalcin may have a direct or indirect influence on energy expenditure. It can also be interpreted as BAT stimulating bone anabolism [43]. Previous papers have shown a correlation between bone structure and BAT [19,44,45]. Moreover, recently it was shown in vitro in mice that osteocalcin in part regulates energy homeostasis by regulating BAT thermogenesis [24]. On the other hand, osteocalcin could also be produced in BAT itself, as it recently was shown in male mice that the osteocalcin gene is upregulated in bone and BAT after cold-stress [23].

After correction for adiposity, a negative correlation between thigh muscle volume and FF in sBAT was found. No correlation was found without correction for adiposity, probably due to positive correlations between adiposity and both thigh muscle volume (correlations in Table S6 in the supplementary materials) and sBAT FF. On the other hand, the correlation found after correction for adiposity could potentially be due to mediation via irisin, fibroblast growth factor 21, interleukin-6, or some other myokine released during physical activity [13], although such hormones were not measured in this study. This finding is in line with a previous retrospective study in children and adolescents, in which a positive association between neck and gluteus muscle volumes and the presence of active BAT was observed [18]. Our findings are also supported by findings in adults, with a positive correlation between active BAT volume and thigh muscle cross sectional area [19]. In contrast, a paper studying young adult men during cold exposure using ^{18}F-FDG PET/CT found that endurance trained individuals had less BAT activity compared to sedentary individuals [16]. A similar study on young adult women found no correlation, but a trend towards less BAT activity in the physically active group [17].

The current findings of BAT in correlation to osteocalcin and thigh muscle volume are interesting as it is since decades known that there is a strong correlation between bone and muscle mass [46]. Further, in mice it has been shown that osteocalcin, during exercise, improves

Table 2
sBAT FF in linear regressions against other measurements, with correction for sex and age (n = 63).

Independent variable	Beta of independent variable [95% confidence interval]	Adjusted R^2	*p*-Value of independent variable	*p*-Values of explanatory variables (sex/age)
Weight [kg]	0.27 [−0.06 0.60]	< 0.01	0.10	(0.82/0.51)
Height [cm]	−0.26 [−0.55 0.02]	0.02	0.068	(0.83/0.22)
WC [cm]	0.37 [0.12 0.63]	0.09	**0.0051**	(0.68/0.60)
BMI [kg/m^2]	1.0 [0.4 1.6]	0.13	**0.0013**	(0.97/0.44)
WHtR	68 [37100]	0.21	**5.8e-05**	(0.82/0.46)
MRI data				
sBAT T_2* [ms]	0.52 [0.04 1.01]	0.04	**0.036**	(0.92/0.67)
sBAT volume [l]	123 [80166]	0.33	**4.1e-07**	(0.80/0.59)
sBAT volume[a] [l]	200 [149251]	0.50	**1.1e-10**	(0.78/0.80)
VAT FF [%]	0.48 [−0.21 1.17]	< 0.01	0.17	(0.88/0.32)
VAT volume [l]	14 [5 23]	0.13	**0.0017**	(0.94/0.32)
VAT volume[a] [l]	23 [11 34]	0.18	**0.00027**	(0.83/0.30)
SAT FF [%]	1.0 [0.6 1.4]	0.25	**2.0e-05**	(0.14/0.36)
SAT volume [l]	4.1 [2.0 6.1]	0.18	**0.00023**	(0.30/0.29)
Thigh muscle volume [l]	−1.0 [−9.2 7.2]	< 0.01	0.81	(0.94/0.36)
Serum analyses				
Insulin [pmol/l]	0.038 [−0.073 0.149]	< 0.01	0.49	(0.87/0.46)
Glucose [mmol/l]	0.63 [−2.59 3.85]	< 0.01	0.69	(0.55/0.69)
Osteocalcin [μg/l]	−0.058 [−0.105–0.011]	0.06	**0.017**	(0.23/0.71)
Adiponectin [mg/l]	−0.060 [−0.347 0.228]	< 0.01	0.68	(0.84/0.50)
Leptin [μg/l]	0.80 [0.29 1.32]	0.11	**0.0029**	(0.18/0.42)

Statistically significant *p*-values in **bold**.
[a] Excluding one extreme outlier, same subject in both cases.

muscle function, promotes muscle uptake and utilization of glucose and fatty acids, and promotes muscle interleukin-6 secretion [47]. The Utah paradigm of skeletal physiology states that bone and muscle form a kind of operational unit. Could the bone-derived osteocalcin be the link between bone, muscle, and BAT? Some findings support the view of BAT and skeletal muscle being synergistic partners [48]. Indeed, as mentioned above, correlations between bone structure and BAT have been reported before [19,44,45,49]. It is possible that BAT stimulates bone anabolism, and that the two tissues communicate via secreted factors [49].

Previous studies in adults have shown a negative association between BAT activity and adiposity [3,4]. Furthermore, sBAT FF has been found to be positively associated with BMI and weight in the age group 9.2–19.0 years [50], and another study on children aged 9–15 years found that obese children showed higher FF in sBAT than normal weight children [51]. In a study on prepubertal children aged 6.5–10.2 years, where measurements of the supraclavicular region by thermal imaging before and after a cold stimulus was used to assess BAT activity, a higher BAT activation associated with a lower amount of visceral fat and with a favorable metabolic profile [52]. With this in mind, the observed positive correlations between sBAT FF and adiposity measurements, including those measured using MRI, in this study were expected. This link is probably due to the mixture of brown and white adipocytes in sBAT and the 'whitening' of brown adipocytes when inactive [53]. The only measures of adiposity that did not correlate with sBAT FF were weight and VAT FF. The lack of a correlation between sBAT FF and weight is probably due to the strong and well known correlation between absolute weight and height (also found in this population, correlation presented in Table S7 in the supplementary materials). The significant correlation between sBAT FF and SAT FF, but not with VAT FF is potentially an indication that the sBAT depot is more closely related to the SAT than to the VAT in this 7 year-old cohort. In rodents, there have been studies that show that SAT is more prone to switch to brown fat-like behavior as a consequence of exercise training than VAT [13], which could be construed as support of this thesis.

Even the highest measured FF in sBAT was lower compared to the lowest value in SAT or VAT in these young children, which indicates the presence of BAT [30–32]. The children in this study had sBAT FFs higher than what has previously been measured in infants [50], but lower than children aged 9.2–19.0 years [50], and even lower compared to adults [31,32,39]. Although it should be noted that it is difficult to compare these values between studies due to methodical differences. There is currently no consensus of how these measurements should be done.

A significant positive correlation between sBAT-FF and sBAT-T_2* was found in this study. A similar finding in children has been reported earlier [50]. This is likely due to both a decreased triglyceride content and an increase of the vascularization and the number of mitochondria in BAT as compared to WAT. This correlation could be seen as an indication that the measured sBAT indeed consists at least partly of BAT.

Previous retrospective studies of pediatric patients that had been scanned using ^{18}F-FDG PET/CT at ambient temperatures found no difference in BAT activity between the sexes [54,55]. One of the studies found a nonlinear correlation between BAT activity and age [54], while the other found that the detection of BAT by ^{18}F-FDG uptake was less

Table 3
sBAT FF in linear regressions against thigh muscle volume and serum analyses, with correction for sex, age, and BMI (n = 63).

Independent variable	Beta of independent variable [95% confidence interval]	Adjusted R^2	*p*-Value of independent variable	*p*-Values of explanatory variables (sex/age/BMI)
Thigh muscle volume [l]	−17 [−26–8]	0.28	**0.00050**	(0.34/**0.041**/**3.6e-06**)
Insulin [pmol/l]	−0.082 [−0.202 0.039]	0.16	0.18	(0.88/0.57/**0.00073**)
Glucose [mmol/l]	0.0045 [−3.0480 3.0570]	0.08	1.00	(0.59/0.58/**0.0073**)
Osteocalcin [μg/l]	−0.054 [−0.097–0.011]	0.22	**0.014**	(0.30/0.69/**0.00063**)
Adiponectin [mg/l]	−0.030 [−0.293 0.233]	0.13	0.82	(0.96/0.47/**0.00085**)
Leptin [μg/l]	0.22 [−0.66 1.09]	0.14	0.62	(0.63/0.44/0.11)

Statistically significant *p*-values in **bold**.

Table 4
sBAT FF in linear regressions against thigh muscle volume and serum analyses, with correction for sex, age, and SAT volume (n = 62).

Independent variable	Beta of independent variable [95% confidence interval]	Adjusted R^2	*p*-value of independent variable	*p*-values of explanatory variables (sex/age/SAT volume)
Thigh muscle volume [l]	−12 [−20–4]	0.28	**0.0045**	(**0.046**/**0.043**/**3.8e-06**)
Insulin [pmol/l]	−0.079 [−0.189 0.032]	0.22	0.16	(0.27/0.40/**8.4e-05**)
Glucose [mmol/l]	−0.78 [−4.01 2.45]	0.14	0.63	(0.17/0.51/**0.0014**)
Osteocalcin [μg/l]	−0.055 [−0.097–0.013]	0.27	**0.011**	(0.92/0.56/**6.7e-05**)
Adiponectin [mg/l]	−0.030 [−0.285 0.225]	0.18	0.81	(0.30/0.35/**0.00017**)
Leptin [μg/l]	−0.086 [−0.900 0.727]	0.19	0.83	(0.24/0.33/**0.010**)

Statistically significant *p*-values in **bold**.

frequent in prepubertal than in pubertal subjects [55]. Sex and age were only significant contributors in a few of the correlations in this study, and even in these cases the *p*-values were relatively high (> 0.04). These significant values could likely be explained by multiple testing. The lack of significance is probably due to that the cohort studied was homogenous. The age range was very narrow and the children prepubertal without influence of sex hormones.

Again, studies in adults using ^{18}F-FDG PET/CT after cold activation has shown a significant impact of BAT on glucose metabolism [9,56]. However, in our study no correlations between sBAT FF and fasting levels of markers related to glucose homeostasis, such as adiponectin, glucose, or insulin, with or without correction for adiposity, were found. The reason for this could be that the studied children are young and relatively healthy, and have not yet developed any severe symptoms of the metabolic syndrome such as increased glucose levels, and in that sense are too homogenous. Interestingly, serum adiponectin did not correlate at all with adiposity in this healthy population (correlations presented in Table S8 in the supplementary materials), and therefore the lack of a correlation to sBAT FF not surprising.

Serum leptin levels and sBAT FF correlated, but not when correction for adiposity was performed. Without adiposity correction, the explanatory power of leptin was lower than that of most measures of adiposity, and leptin is known to correlate well with adiposity both in children [57] and in adults [58], and did so in this study as well (correlation presented in Table S9 in the supplementary materials). This likely explains the lack of a correlation when correcting for adiposity.

As mentioned in Section 1, some studies have found negative correlations between sBAT FF and glucose uptake rate of the sBAT depot during cooling [33,34], while another study failed to find such a correlation [35]. While it is likely that the sBAT FF to some degree reflects the tissue's potential for cold activated energy expenditure, it is not a certainty.

Finally, it should be noted that the study is limited in that the whole-body protocol employed was not optimized for measuring the FF of sBAT, VAT, or SAT. A protocol designed for this could potentially result in stronger correlations. Further, it was noted that the T_2* in the sBAT area measurements varied considerably, with some voxels having extremely high values, but more voxels having extremely low values. It is therefore likely that the calculated T_2* values were underestimated. An additional weakness is that the MRI examinations were performed approximately half a year after the anthropometric measurements and blood sampling. This may have weakened the correlations. Since BAT

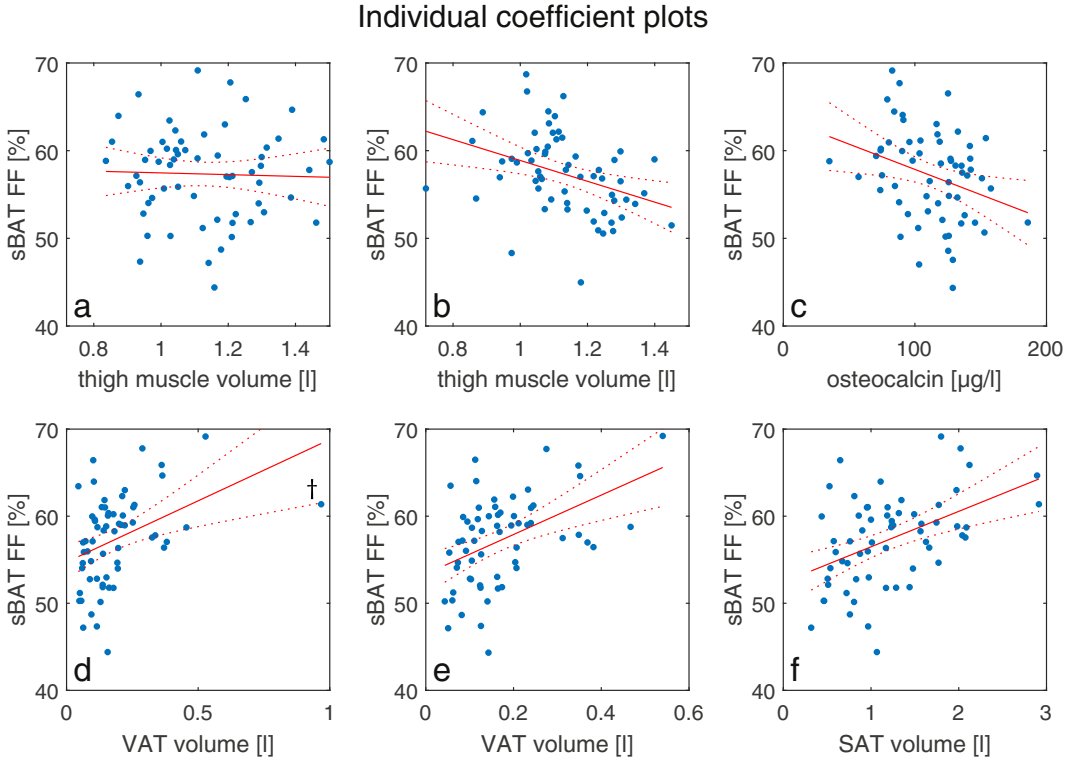

Fig. 2. Individual coefficient plots for the measurements indicated along the x-axis against sBAT FF. The solid lines represent fitted regression lines and the dotted curves represent the corresponding 95% confidence bounds. All values are adjusted for sex and age, additionally, the values in plot **b** are adjusted for SAT volume. All plots include all data points, except for plot **e**, which excludes an outlier with an extreme VAT volume, indicated with † in plot **d**.

and WAT co-exist in the sBAT depot, the measured values most likely do not purely reflect upon the properties of the brown adipocytes. This problem would exist even if ^{18}F-FDG scans were available to use as a reference, although it could possibly be mitigated to some degree by focusing the measurements in the areas with a higher ^{18}F-FDG uptake.

5. Conclusions

It was found that whole-body water-fat MRI of children allows for measurements of sBAT. The FF of sBAT was lower than that of VAT and SAT, indicating presence of BAT. Expected positive associations between sBAT FF and adiposity measurements, including serum leptin levels, were found. Additionally, a negative association to thigh muscle volume after adiposity correction and a negative association to osteocalcin concentration, with and without correction for adiposity, were found. This could imply a hormonal active BAT.

Supplementary data to this article can be found online at https://doi.org/10.1016/j.mri.2019.02.001.

Declarations of interest

None.

Grant support

The sponsor had no role in study design, collection, analysis or interpretation of data, in the writing of this report or the decision to submit the article for publication.

Funding

This research project was supported financially by grants from the Swedish Research Council (2013-3013 and 2016-01040), the Halland County Council, and the Västra Götaland Region.

Acknowledgments

We thank the children and their parents who participated and our research nurses Eivor Kjellberg, Monika Nygren, and Ann-Katrine Karlsson. We thank Per-Arne Svensson for his skills during the MR-examinations and help in designing the MRI protocols. We thank Linnéa Bergman for her assistance during the examinations and Anders Holmén for database management support. We also thank Eira Stokland as the head of radiology unit for her involvement in co-designing the study.

References

[1] Yoneshiro T, Aita S, Matsushita M, Okamatsu-Ogura Y, Kameya T, Kawai Y, et al. Age-related decrease in cold-activated brown adipose tissue and accumulation of body fat in healthy humans. Obesity 2011;19(9):1755–60.
[2] Lidell ME, Betz MJ, Dahlqvist Leinhard O, Heglind M, Elander L, Slawik M, et al. Evidence for two types of brown adipose tissue in humans. Nat Med 2013;19(5):631–4.
[3] Vijgen GH, Bouvy ND, Teule GJ, Brans B, Schrauwen P, van Marken Lichtenbelt WD. Brown adipose tissue in morbidly obese subjects. PLoS One 2011;6(2):e17247.
[4] van Marken Lichtenbelt WD, Vanhommerig JW, Smulders NM, Drossaerts JMAFL, Kemerink GJ, Bouvy ND, et al. Cold-activated brown adipose tissue in healthy men. N Engl J Med 2009;360(15):1500–8.
[5] Frühbeck G, Becerril S, Sáinz N, Garrastachu P, García-Velloso MJ. BAT: a new target for human obesity? Trends Pharmacol Sci 2009;30(8):387–96.
[6] Kershaw EE, Flier JS. Adipose tissue as an endocrine organ. J Clin Endocrinol Metab 2004;89(6):2548–56.
[7] Villarroya F, Cereijo R, Villarroya J, Giralt M. Brown adipose tissue as a secretory organ. Nat Rev Endocrinol 2017;13(1):26–35.
[8] Orava J, Nuutila P, Lidell ME, Oikonen V, Noponen T, Viljanen T, et al. Different metabolic responses of human brown adipose tissue to activation by cold and insulin. Cell Metab 2011;14(2):272–9.
[9] Chondronikola M, Volpi E, Børsheim E, Porter C, Annamalai P, Enerbäck S, et al. Brown adipose tissue improves whole-body glucose homeostasis and insulin sensitivity in humans. Diabetes 2014;63(12):4089–99.
[10] Morrison SF, Madden CJ, Tupone D. Central control of brown adipose tissue thermogenesis. Front Endocrinol 2012;3:5.
[11] López M, Nogueiras R, Tena-Sempere M, Diéguez C. Hypothalamic AMPK: a canonical regulator of whole-body energy balance. Nat Rev Endocrinol 2016;12(7):421–32.
[12] Wei Q, Lee JH, Wang H, Bongmba OYN, Wu C-H, Pradhan G, et al. Adiponectin is required for maintaining normal body temperature in a cold environment. BMC Physiol 2017;17(1):8.
[13] Rodríguez A, Becerril S, Ezquerro S, Méndez-Giménez L, Frühbeck G. Crosstalk between adipokines and myokines in fat browning. Acta Physiol 2017;219(2):362–81.
[14] Boström P, Wu J, Jedrychowski MP, Korde A, Ye L, Lo JC, et al. A PGC1α-dependent myokine that drives browning of white fat and thermogenesis. Nature 2012;481(7382):463–8.
[15] De Matteis R, Lucertini F, Guescini M, Polidori E, Zeppa S, Stocchi V, et al. Exercise as a new physiological stimulus for brown adipose tissue activity. Nutr Metab Cardiovasc Dis 2013;23(6):582–90.
[16] Vosselman MJ, Hoeks J, Brans B, Pallubinsky H, Nascimento EBM, van der Lans AAJJ, et al. Low brown adipose tissue activity in endurance-trained compared with lean sedentary men. Int J Obes (Lond) 2015;39(12):1696–702.
[17] Singhal V, Maffazioli GD, Ackerman KE, Lee H, Elia EF, Woolley R, et al. Effect of chronic athletic activity on brown fat in young women. PLoS One 2016;11(5):e0156353.
[18] Gilsanz V, Chung SA, Jackson H, Dorey FJ, Hu HH. Functional brown adipose tissue is related to muscle volume in children and adolescents. J Pediatr 2011;158(5):722–6.
[19] Bredella MA, Gill CM, Rosen CJ, Klibanski A, Torriani M. Positive effects of brown adipose tissue on femoral bone structure. Bone 2014;58:55–8.
[20] Hauschka PV, Lian JB, Cole DE, Gundberg CM. Osteocalcin and matrix Gla protein: vitamin K-dependent proteins in bone. Physiol Rev 1989;69(3):990–1047.
[21] Zoch ML, Clemens TL, Riddle RC. New insights into the biology of osteocalcin. Bone 2016;82:42–9.
[22] Kalra SP, Dube MG, Iwaniec UT. Leptin increases osteoblast-specific osteocalcin release through a hypothalamic relay. Peptides 2009;30(5):967–73.
[23] Camerino C, Conte E, Caloiero R, Fonzino A, Carratù M, Lograno MD, et al. Evaluation of short and long term cold stress challenge of nerve grow factor, brain-derived neurotrophic factor, osteocalcin and oxytocin mRNA expression in BAT, brain, bone and reproductive tissue of male mice using real-time PCR and linear correlation analysis. Front Physiol 2018;8:1101.
[24] Li Q, Hua Y, Yang Y, He X, Zhu W, Wang J, et al. TCF7/TCF1 feedback controls osteocalcin signaling in brown adipocytes independent of canonical WNT/β-catenin pathway. Mol Cell Biol 2018;38(7). (e00562-17).
[25] Luo X-H, Guo L-J, Yuan L-Q, Xie H, Zhou H-D, Wu X-P, et al. Adiponectin stimulates human osteoblasts proliferation and differentiation via the MAPK signaling pathway. Exp Cell Res 2005;309(1):99–109.
[26] Polgreen LE, Jacobs Jr. DR, Nathan BM, Steinberger J, Moran A, Sinaiko AR. Association of osteocalcin with obesity, insulin resistance, and cardiovascular risk factors in young adults. Obesity 2012;20(11):2194–201.
[27] Cypess AM, Lehman S, Williams G, Tal I, Rodman D, Goldfine AB, et al. Identification and importance of brown adipose tissue in adult humans. N Engl J Med 2009;360(15):1509–17.
[28] Virtanen KA, Lidell ME, Orava J, Heglind M, Westergren R, Niemi T, et al. Functional brown adipose tissue in healthy adults. N Engl J Med 2009;360(15):1518–25.
[29] Saito M, Okamatsu-Ogura Y, Matsushita M, Watanabe K, Yoneshiro T, Nio-Kobayashi J, et al. High incidence of metabolically active brown adipose tissue in healthy adult humans: effects of cold exposure and adiposity. Diabetes 2009;58(7):1526–31.
[30] Hu HH, Perkins TG, Chia JM, Gilsanz V. Characterization of human brown adipose tissue by chemical-shift water-fat MRI. AJR Am J Roentgenol 2013;200(1):177–83.
[31] Gifford A, Towse TF, Walker RC, Avison MJ, Welch EB. Characterizing active and inactive brown adipose tissue in adult humans using PET-CT and MR imaging. Am J Physiol Endocrinol Metab 2016;311(1):E95–104.
[32] Jones TA, Wayte SC, Reddy NL, Adesanya O, Dimitriadis GK, Barber TM, et al. Identification of an optimal threshold for detecting human brown adipose tissue using receiver operating characteristic analysis of IDEAL MRI fat fraction maps. Magn Reson Imaging 2018;51:61–8.
[33] Holstila M, Pesola M, Saari T, Koskensalo K, Raiko J, Borra RJH, et al. MR signal-fat-fraction analysis and T_2* weighted imaging measure BAT reliably on humans without cold exposure. Metabolism 2017;70:23–30.
[34] Koskensalo K, Raiko J, Saari T, Saunavaara V, Eskola O, Nuutila P, et al. Human brown adipose tissue temperature and fat fraction are related to its metabolic activity. J Clin Endocrinol Metab 2017;102(4):1200–7.
[35] Deng J, Neff LM, Rubert NC, Zhang B, Shore RM, Samet JD, et al. MRI characterization of brown adipose tissue under thermal challenges in normal weight, overweight, and obese young men. J Magn Reson Imaging 2018;47(4):936–47.
[36] Kjellberg E, Roswall J, Bergman S, Strandvik B, Dahlgren J. Serum n-6 and n-9 fatty acids correlate with serum IGF-1 and growth up to 4 months of age in healthy infants. J Pediatr Gastroenterol Nutr 2018;66(1):141–6.
[37] Cole TJ, Lobstein T. Extended international (IOTF) body mass index cut-offs for thinness, overweight and obesity. Pediatr Obes 2012;7(4):284–94.
[38] Tanner JM, Whitehouse RH. Clinical longitudinal standards for height, weight, height velocity, weight velocity, and stages of puberty. Arch Dis Child 1976;51(3):170–9.
[39] Lundström E, Strand R, Johansson L, Bergsten P, Ahlström H, Kullberg J. Magnetic resonance imaging cooling-reheating protocol indicates decreased fat fraction via

lipid consumption in suspected brown adipose tissue. PLoS One 2015;10(4):e0126705.
[40] Otsu N. A threshold selection method from gray-level histograms. IEEE Trans Syst Man Cybern 1979;9(1):62–6.
[41] Kullberg J, Hedström A, Brandberg J, Strand R, Johansson L, Bergström G, et al. Automated analysis of liver fat, muscle and adipose tissue distribution from CT suitable for large-scale studies. Sci Rep 2017;7(1):10425.
[42] Velleman PF, Welsch RE. Efficient computing of regression diagnostics. Am Stat 1981;35(4):234–42.
[43] Rahman S, Lu Y, Czernik PJ, Rosen CJ, Enerbäck S, Lecka-Czernik B. Inducible brown adipose tissue, or beige fat, is anabolic for the skeleton. Endocrinology 2013;154(8):2687–701.
[44] Lee P, Brychta RJ, Collins MT, Linderman J, Smith S, Herscovitch P, et al. Cold-activated brown adipose tissue is an independent predictor of higher bone mineral density in women. Osteoporos Int 2013;24(4):1513–8.
[45] Ponrartana S, Aggabao PC, Hu HH, Aldrovandi GM, Wren TAL, Gilsanz V. Brown adipose tissue and its relationship to bone structure in pediatric patients. J Clin Endocrinol Metab 2012;97(8):2693–8.
[46] Frost HM, Schönau E. The "muscle-bone unit" in children and adolescents: a 2000 overview. J Pediatr Endocrinol Metab 2000;13(6):571–90.
[47] Mera P, Laue K, Ferron M, Confavreux C, Wei J, Galán-Díez M, et al. Osteocalcin signaling in myofibers is necessary and sufficient for optimum adaptation to exercise. Cell Metab 2016;23(6):1078–92.
[48] Bal NC, Maurya SK, Pani S, Sethy C, Banerjee A, Das S, et al. Mild cold induced thermogenesis: are BAT and skeletal muscle synergistic partners? Biosci Rep 2017;37(5):BSR20171087.
[49] Lidell ME, Enerbäck S. Brown adipose tissue and bone. Int J Obes Suppl 2015;5(S1):S23–7.
[50] Hu HH, Yin L, Aggabao PC, Perkins TG, Chia JM, Gilsanz V. Comparison of brown and white adipose tissues in infants and children with chemical-shift-encoded water-fat MRI. J Magn Reson Imaging 2013;38(4):885–96.
[51] Deng J, Schoeneman SE, Zhang H, Kwon S, Rigsby CK, Shore RM, et al. MRI characterization of brown adipose tissue in obese and normal-weight children. Pediatr Radiol 2015;45(11):1682–9.
[52] Malpique R, Gallego-Escuredo JM, Sebastiani G, Villarroya J, López-Bermejo A, de Zegher F, et al. Brown adipose tissue in prepubertal children: associations with sex, birthweight, and metabolic profile. Int J Obes (Lond) 2018. https://doi.org/10.1038/s41366-018-0198-7.
[53] Heaton JM. The distribution of brown adipose tissue in the human. J Anat 1972;112(Pt 1):35–9.
[54] Drubach LA, Palmer EL, Connolly LP, Baker A, Zurakowski D, Cypess AM. Pediatric brown adipose tissue: detection, epidemiology, and differences from adults. J Pediatr 2011;159(6):939–44.
[55] Gilsanz V, Smith ML, Goodarzian F, Kim M, Wren TAL, Hu HH. Changes in brown adipose tissue in boys and girls during childhood and puberty. J Pediatr 2012;160(4):604–9.
[56] Matsushita M, Yoneshiro T, Aita S, Kameya T, Sugie H, Saito M. Impact of brown adipose tissue on body fatness and glucose metabolism in healthy humans. Int J Obes (Lond) 2014;38(6):812–7.
[57] Arslanian S, Suprasongsin C, Kalhan SC, Drash AL, Brna R, Janosky JE. Plasma leptin in children: relationship to puberty, gender, body composition, insulin sensitivity, and energy expenditure. Metabolism 1998;47(3):309–12.
[58] Considine RV, Sinha MK, Heiman ML, Kriauciunas A, Stephens TW, Nyce MR, et al. Serum immunoreactive-leptin concentrations in normal-weight and obese humans. N Engl J Med 1996;334(5):292–5.